Analysis of Power Holes in Helix Traveling-Wave Tubes with Non-Uniform Delay-Lines

***Moritz Hägermann*[1], *Michael Wulff*[1], *Philip Birtel*[2], and *Arne F. Jacob*[1]**

[1]Institute of High-Frequency Technology, Hamburg University of Technology, Hamburg, Germany

[2]Thales Deutschland GmbH, Electron Devices, Ulm, Germany

Contact: moritz.haegermann@tuhh.de

Abstract

The influence of non-uniform delay lines on the parasitic effect of power holes in helix traveling-wave tubes is investigated. For the analysis, we introduce a helix geometry which favors power hole occurrence. The harmonic backward-wave is assumed to be excited through output-coupler mismatch. Whereas homogeneous delay lines can only cause a single power hole, the analysis shows that tapered helices may lead to multiple gain dips at different frequencies where each power hole can be assigned to a section of the delay line.

INTRODUCTION

Power holes are narrowband gain degradations in helix traveling-wave tubes (TWTs). The nonlinear amplifier characteristics lead to the generation of drive-frequency harmonics at which the delay-line couplers or external loads are often poorly matched. Thus, backward waves are introduced by reflections, e.g., at the output coupler, and amplified if synchronism with the slow space-charge wave of the electron beam is given. As a consequence, the drive-signal amplification is reduced in a narrowband frequency region, commonly called power hole.

Power holes in homogeneous delay-lines have been analyzed in simulation and verified by measurements in [1] and [2] where also suppression techniques have been included. The present contribution deals with the influence of non-uniform helical delay-lines, as they are widely used in high-efficiency helix TWTs.

After a brief introduction to the fundamentals of power holes, a model generated for the simulation of power holes is developed. Finally, simulation results are presented and discussed.

FUNDAMENTALS OF POWER HOLES

In helix TWTs, the electron beam is synchronous with the fundamental spatial harmonic of the forward wave and, in addition, with the first negative spatial harmonic of the backward wave [3]. The former enables broadband amplification of the drive signal, which is the intended operating mode of the TWT. In the latter case, narrowband backward-wave amplification occurs and can even lead to instabilities, known as backward-wave oscillations.

In the case of power holes, the harmonic at $2f_0$ of the drive-signal frequency f_0 falls within the range of backward-wave interaction as shown in the dispersion diagram in Figure 1. In the nonlinear saturation region of the TWT, backward waves are introduced by reflections of the forward wave's harmonic. From the gain competition of the waves follows a narrowband gain degradation at f_0.

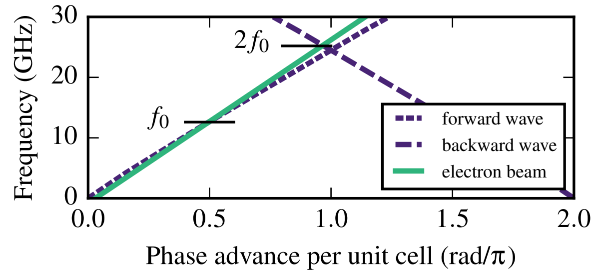

Figure 1. Dispersion of the helix and the beam line.

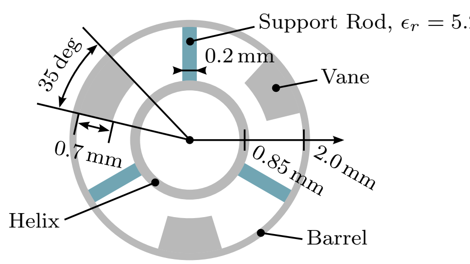

Figure 2. Delay-line cross-section.

Whereas the delay-line couplers, discontinuities of the delay line itself, or severs are usually well matched at f_0, they often introduce strong reflections at $2f_0$ as the delay-line impedance changes significantly with frequency [4]. Here, only output-coupler reflections are taken into account as they represent the dominant contributor. Thus, simulation has to fulfill the boundary condition at the end of the interaction region

$$P_{\mathrm{BW},2f_0} = \Gamma^2 \cdot P_{\mathrm{FW},2f_0}, \tag{1}$$

where Γ is the reflection coefficient, and $P_{\mathrm{FW},2f_0}$ and $P_{\mathrm{BW},2f_0}$ are the RF wave powers at $2f_0$ of the forward and backward wave, respectively.

Although power holes can be prevented by modifying the helix geometry and consequently shifting the backward-wave interaction frequency away from the drive signal's harmonic, this might not always be feasible in ultra-broadband TWTs with several octaves of bandwidth.

TWT MODEL

In this work, the analysis is performed for a generic helical delay-line as shown in Figure 2, where the support rods

978-1-5386-8288-3/20/$31.00 ©2020 IEEE

are assumed to be lossless and a distributed attenuation of $0.13\,\mathrm{dB}/\lambda$ takes helix losses into account. The electron beam ($6.9\,\mathrm{kV}$, $100\,\mathrm{mA}$) is focused by a homogeneous magnetic field of $1400\,\mathrm{G}$. The tube is driven at saturation and the boundary condition from Equation (1) holds. According to Figure 1, this configuration enables the generation of power holes. Additionally, it is ensured that a π-mode oscillation is not likely to occur as it possibly arises due to beam-wave synchronism close to the π-point.

POWER HOLES IN NON-UNIFORM DELAY-LINES

High-performance TWTs commonly use non-uniform delay-lines with a pitch profile similar to the one presented in [5]. Figure 3 shows the model's pitch profile. The delay line has an overall length of 130 mm. Attenuators and severs are omitted to simplify the analysis. The helix consists of three homogeneous sections in the intervals (0 mm, 45 mm), (55 mm, 80 mm) and (85 mm, 95 mm).

Figure 4 reports simulation results which were obtained with MVTRAD3D [6]. It shows the drive-signal gain for various reflection coefficients. This includes the matched case ($\Gamma = 0$) for comparison. For $\Gamma^2 = 0.5$, three power holes, marked with f_1, f_2, and f_3, are found, each with a gain degradation of approximately $0.65\,\mathrm{dB}$. The depth of the power holes scales with the reflection coefficient as can be seen from the gain curves for $\Gamma^2 = 0.2$ and $\Gamma^2 = 0.8$. The slight gain degradations at f_4 and f_5 result from the interaction with the fast space-charge wave. Although the backward-wave is attenuated here, the beam gets modulated which disturbs the drive-signal amplification.

To clarify the gain dips, Figure 3 also shows the corresponding backward-wave powers at $2f_i$ versus z, with $i = 1, 2, \ldots 6$. At $2f_1$, $2f_2$, and $2f_3$ all waves are amplified in a certain helix section as exemplarily marked by the arrow for $2f_3$. As the waves travel from the collector end towards the gun, they are amplified as indicated by the power increase. Each power hole can thus be assigned to a homogeneous helix section, i.e., f_3 to the first, f_2 to the second, and f_1 to the third helix section. The power hole frequencies correlate with the individual backward-wave phase velocities in the corresponding helix sections. At $2f_4$ and $2f_5$ the backward waves are more strongly attenuated compared to the asynchronous case at $2f_6$, which is caused by beam-wave interaction with the fast space-charge wave. Attenuation at $2f_6$ only results from the helix losses.

CONCLUSION

A TWT model is presented to evaluate the effect of power holes in non-uniform delay-lines. Compared to uniform delay-lines, each homogeneous helix-section causes a power hole in the case of tapered helices as shown here. Depending on the application, this might lead to a significant performance degradation. The backward wave does not only interact with the slow space-charge wave, but also with the fast one. This modulates the electron beam and distorts the amplification process.

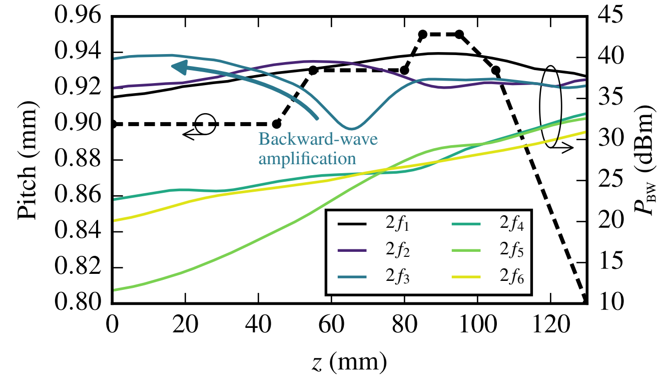

Figure 3. Pitch profile and backward-wave powers versus z.

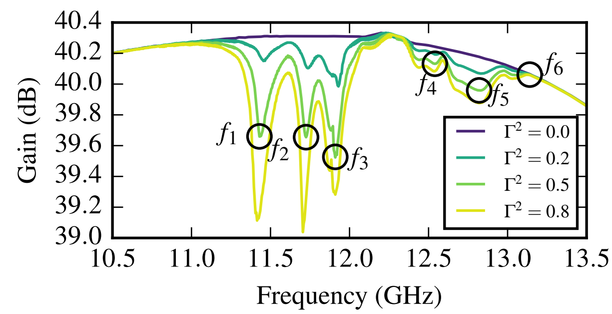

Figure 4. Gain for different reflection-coefficients.

ACKNOWLEDGMENT

The authors wish to acknowledge funding and support of this work by the German Aerospace Center (DLR) on behalf of the German Federal Ministry of Economics and Technology (BMWi) under research contract 50YB1712.

REFERENCES

[1] D. Chernin, T. M. Antonsen, Jr., and Baruch Levush, "“Power Holes” and Nonlinear Forward and Backward Wave Gain Competition in Helix Traveling-Wave Tubes," in *IEEE Trans. Electron Devices*, vol. 50, 2003, pp. 2540–2547.

[2] Y. Gong, Z. Duan, Y. Wang, Y. Wei, H. Yin, and W. Wang, "Suppression of In-Band Power Holes in Helix Traveling-Wave Tubes," in *IEEE Trans. Electron Devices*, vol. 58, 2011, pp. 1556–1561.

[3] J. R. Pierce, "Traveling-Wave Tubes," *D. van Nostrand Company, Inc.*, 1950, ch. XI.

[4] A. S. Gilmour, Jr., "Principles of Traveling Wave Tubes," *Artech House, Inc.*, 1994, pp. 334–337.

[5] D. K. Abe, B. Levush, T. M. Antonsen, Jr., D. R. Whaley, and B. G. Danly, "Design of a Linear C-Band Helix TWT for Digital Communications Experiments Using the CHRISTINE Suite of Large-Signal Codes," in *IEEE Trans. Plasma Science*, vol. 30, 2002, pp. 1053–1062.

[6] J.-F. David and D. Bariou, "A 3D Large Signal Model for Helix TWT," in *2013 IEEE Int. Vacuum Electronics Conf.*.